

Metal-Metal Redox Exchange to Produce Heterometallic Manganese-Cobalt Oxo Cubanes *via* a “Dangler” Intermediate

T. Alexander Wheeler^[a,b] and T. Don Tilley*^[a,b]

^[a]Department of Chemistry, University of California, Berkeley, Berkeley, California 94720, United States

^[b]Chemical Sciences Division, Lawrence Berkeley National Laboratory, Berkeley, California 94720, United States

Abstract: Pendent metals bound to heterocubanes are key components of well-known active sites in enzymes that mediate difficult chemical transformations. Investigations into the specific role of these metal ions, sometimes referred to as “danglers,” have been hindered by a paucity of rational synthetic routes to appropriate model structures. To generate pendent metal ions bonded to an oxo cubane through a carboxylate bridge, the cubane $\text{Co}_4(\mu_3\text{-O})_4(\text{OAc})_4(t\text{-Bupy})_4$ (OAc = acetate, *t*-Bupy = 4-*tert*-butylpyridine) was exposed to various metal acetate complexes. Reaction with $\text{Cu}(\text{OAc})_2$ gave the structurally characterized (by X-ray diffraction) dicopper dangler $\text{Cu}_2\text{Co}_4(\mu_4\text{-O})_2(\mu_3\text{-O})_2(\text{OAc})_6(\text{Cl})_2(t\text{-Bupy})_4$. In contrast, the analogous reaction with $\text{Mn}(\text{OAc})_2$ produced the Mn^{IV}-containing cubane cation $[\text{MnCo}_3(\mu_3\text{-O})_4(\text{OAc})_4(t\text{-Bupy})_4]^+$ by way of a metal-metal exchange that gives $\text{Co}(\text{OAc})_2$ and $[\text{Co}^{\text{III}}(\mu\text{-OH})(\text{OAc})]_n$ oligomers as byproducts. Additionally, reaction of the formally Co^{IV} cubane complex $[\text{Co}_4(\mu_3\text{-O})_4(\text{OAc})_4(t\text{-Bupy})_4][\text{PF}_6]$ with $\text{Mn}(\text{OAc})_2$ gave the corresponding Mn-containing cubane in 80% yield. A kinetic and mechanistic examination of the related metal-metal exchange reaction between $\text{Co}_4(\mu_3\text{-O})_4(\text{OBz})_4(\text{py})_4$ (OBz = benzoate) and $[\text{Mn}(\text{acac})_2(\text{py})_2][\text{PF}_6]$ by UV-vis spectroscopy provided support for a process involving rate-determining association of the reactants and electron transfer through a μ -oxo bridge in the adduct intermediate. The rates of exchange correlate with the donor strength of the cubane pyridine and benzoate ligand substituents; more electron-donating pyridine ligands accelerate metal-metal exchange, while both electron donating and withdrawing benzoate ligands can accelerate exchange. These experiments suggest that the basicity of the cubane oxo ligands promotes metal-metal exchange reactivity. The redox potentials of the Mn and cubane starting materials, and isotopic labeling studies, suggest an inner-sphere electron transfer mechanism in a dangler intermediate.

Introduction

Tetrametallic tetrachalcogenide heterocubane clusters (M_4E_4 , E = O, S) are important reaction centers that effectively mediate proton-coupled, multi-electron chemical processes in biological systems.¹⁻⁴ Prominent examples include $[\text{Fe}_4\text{S}_4]$ iron sulfur clusters that are essential electron-transfer cofactors for a range of enzymes.⁵⁻⁷ The CaMn_4O_4 cluster known as the oxygen evolving complex (OEC, Figure 1a) of Photosystem II, and the NiFe_4S_4 active site of carbon monoxide dehydrogenase (CODH) are structurally similar heterocubane complexes that play an important role in enzymatic catalysis.⁸ The importance of this structural motif in biology has motivated significant research into the role of the tetrametallic assembly, and much of this effort has benefited from the use of synthetic models that mimic structural and spectroscopic aspects of the appropriate cubane.^{5, 9-11} Indeed, synthetic models were instrumental in establishing the basic geometry of the OEC before high resolution X-ray diffraction enabled determination of the active site arrangement.¹²⁻¹⁴ Current OEC model systems effectively replicate EPR spectra observed for the S2 and S3 state of the OEC, and structurally reproduce nearly all of the key OEC bonding motifs (Figure 1b).¹⁵⁻²⁴ Despite the progress made from these studies, the synthesis of cubane models that accurately mimic biological function remains a significant challenge, in part due to a limited understanding of cubane assembly mechanisms. Investigations into the assembly and metal-metal exchange reactivity of iron sulfur clusters has demonstrated that these clusters can readily undergo Fe-Fe exchange, as shown by isotopic labeling studies.²⁵⁻²⁹ However, general synthetic methods that allow construction of heterometallic cubanes analogous to those observed in biology are quite limited, and the mechanisms by which heterocubanes assemble remain poorly understood.³⁰⁻³⁴

An interesting feature of certain cubane active sites is their close association with an additional redox-active metal ion that is directly involved in the function of the enzyme.⁸ In the OEC, a CaMn_3O_4 oxo cubane is associated with a pendent Mn ion referred to as the “dangler” (Figure 1a), whereas an Fe_3NiS_4 cubane of the CODH active site is bound to an Fe ion.^{35, 36} In proposed catalytic mechanisms for both the OEC and CODH, these exogenous metal ions directly assist in utilizing accumulated redox equivalents of the cubane to perform difficult reactions at low overpotentials.³⁷⁻⁴³ Despite clear indication that these dangler ions are essential, a detailed mechanistic understanding of their specific role is lacking.

Therefore, an important research objective is the preparation and study of cubane model systems that possess redox-active, dangler metal centers. Only a few dangler-cubane assemblies have been synthesized (e.g., Figure 1b,c), including a manganese-cobalt oxo cubane synthesized by complexation of "Co^{II}(NO₃)(OAc)" to the oxo cubane MnCo₃(μ₃-O)₄(OAc)₅(py)₃ (OAc = acetate, py = pyridine).^{19, 20, 44-46} In this synthesis, an acetate migration assists in complexation of the incoming metal ion to produce a new, κ¹,κ¹-(OAc)MOM' binding mode that supports the dangler structure (Figure 1c). Thus, it appeared that a reasonable starting point for the synthesis of other dangler complexes could involve established oxo cubanes such as Co₄(μ₃-O)₄(OAc)₄(py)₄ in reactions of acetate-containing sources of a dangler ion.⁴⁷

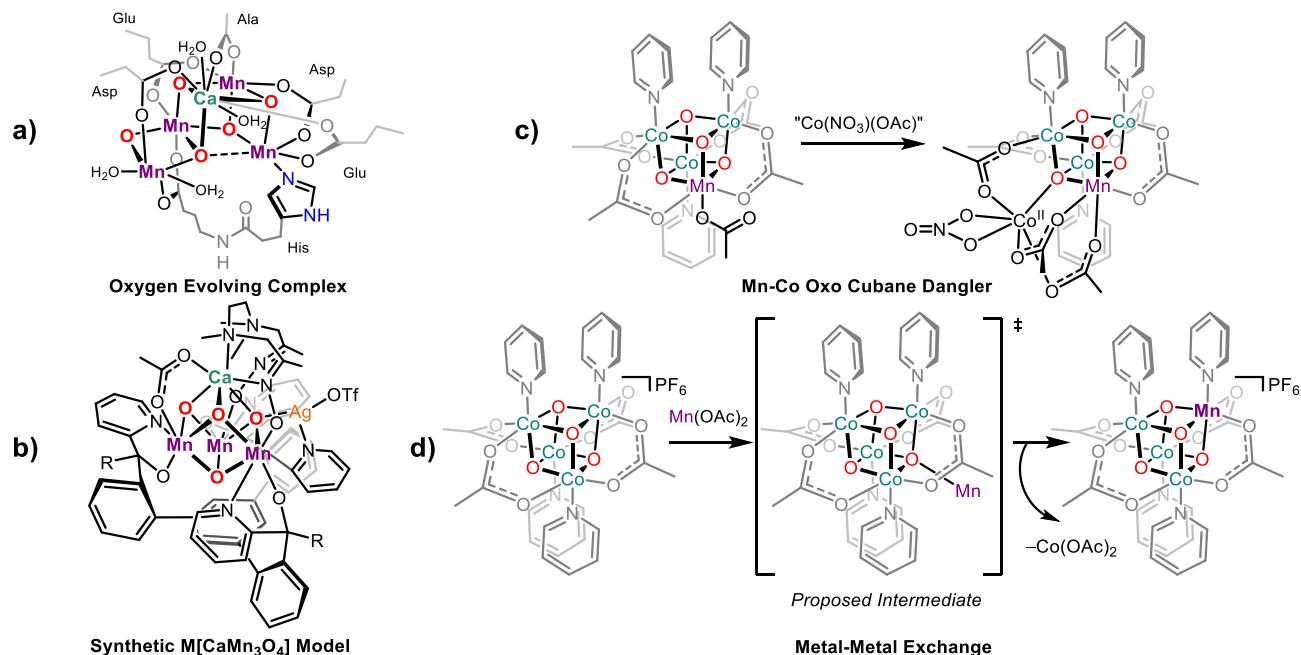


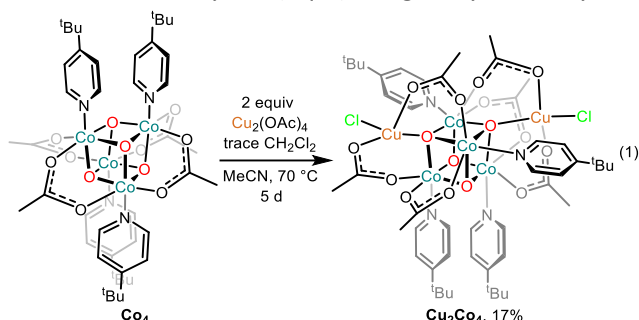
Figure 1. Established metal oxo cubane "dangler" complexes. (a) The oxygen evolving complex (OEC) of Photosystem II. (b) A pentametallic structural analogue of the OEC. (c) A pentametallic model of the OEC complex. (d) Generalized exchange reaction described in this contribution.

This contribution describes the application of this strategy to investigate incorporation of divalent metal ions as danglers onto a cobalt oxo cubane ([Co₄O₄]) core (Scheme 1d). A dangler complex containing two Cu^{II} ions has been discovered, as well as an unexpected metal-metal (Co-Mn) exchange reaction that provides a convenient route to heterometallic oxo cubanes with a manganese-cobalt oxo cubane ([MnCo₃O₄]) core.⁴⁴ As shown herein, this exchange likely occurs through a dangler intermediate possessing acetate-bridged Co and Mn centers. This redox-based exchange process incorporating a Mn^{IV} ion is possibly relevant to the mechanism of biosynthesis of the OEC, which is believed to require multiple Mn^{II} ion oxidation events and a conformational rearrangement in order to generate a Mn₂Ca OEC precursor.^{27, 30, 48, 49} This process may generally point the way to synthesis of new heterometallic cubane complexes, and may also serve as a molecular model for "Galvanic exchange" processes used for doping metal oxide nanoparticles and bulk materials.⁵⁰⁻⁵⁴

Results and Discussion

Synthesis of an Oxo Cubane with Pendent Copper Centers. The possible binding of a monometallic "dangler" metal ion to the oxo cubane cluster, Co₄O₄(OAc)₄(*t*-Bupy)₄ (Co₄, *t*-Bupy = 4-*tert*butylpyridine), was investigated by screening its reactions with divalent transition metal acetates. This approach was motivated by the prior observation that "Co(OAc)(NO₃)" adds to a [MnCo₃O₄] cubane to produce the MnCo₄O₄(OAc)₆(NO₃)(py)₃ dangler complex (Figure 1c).⁴⁴ In the latter process, a bridging acetate ligand detaches from the cubane core to capture the additional metal ion, and this hemilability serves as a pathway to the dangler complex.

Treatment of cubane **Co₄** with Ca(OAc)₂, Fe(OAc)₂, Ni(OAc)₂, or Zn(OAc)₂ in MeCN solution at 23 °C or 55 °C led to complex reaction mixtures that did not appear to contain a dangler complex, as determined by ¹H NMR spectroscopy and high-resolution electrospray ionization mass spectrometry (HR-ESI-MS). However, when a solution of **Co₄** and Cu₂(OAc)₄(H₂O)₂ in MeCN solution (with trace CH₂Cl₂ as solvent of crystallization for **Co₄**) was heated at 70 °C for 16 h, followed by cooling to 23 °C, dark green crystals of paramagnetic Cu₂Co₄(μ₄-O)₂(μ₃-O)₂(OAc)₆Cl₂(*t*-Bupy)₄ (**Cu₂Co₄**) were obtained in 17% yield (eq 1). Single-crystal X-ray diffraction (SC-XRD) analysis enabled determination of the solid-state



molecular structure, which may be described as a “double dangler” complex, with each copper atom bound to a bridging oxo ligand of the cubane (to create two μ₄-oxos) and linked to the cubane core by two bridging acetates. Presumably the chloride ligands on copper originate from the CH₂Cl₂ present in samples of **Co₄**. Thus, the reaction results in retention of the original cubane ligands, and formal addition of two “CuCl(OAc)” units to adjacent corners of the cubane. The resulting cluster displays approximate C₂ symmetry that relates the two four-coordinate Cu centers.

The ¹H NMR spectrum of complex **Cu₂Co₄** in acetonitrile-*d*₃ is consistent with the desymmetrization of **Co₄** (Figure S6); however, the broad paramagnetic resonances cannot definitively confirm the structure. This bonding arrangement is accompanied by exchange of acetate and pyridine coordination sites for two of the Co centers, to produce the observed heterobimetallic CoOCu(1κ²,2κ²-OAc) chelate rings. Binding of the Cu ions results in slight elongation of the Co–O(oxo) bonds (1.89(2) Å) with respect to those for Co₄(μ₃-O)₄(OAc)₄(py)₄ (1.86(2) Å), and all Co–(μ₄-O) distances are elongated to an average of 1.906(6) Å. The solution magnetic moment of 3.3 μ_B (Evans method⁵⁵) is consistent with two isolated Cu^{II} centers.

Cyclic voltammetry of compound **Cu₂Co₄** in MeCN reveals a reversible oxidation at 1.05 V vs. ferrocene/ferrocenium (Figure S8). Interestingly, the binding of the copper fragments increases the oxidation potential of the parent cubane **Co₄** by 0.77 V. Sweeping cathodically reveals a host of overlapping, irreversible reduction events that could not be assigned.

Mn-Co Exchange in Cobalt Oxo Cubane Co₄. The isolation of complex **Cu₂Co₄** suggested that other metal acetates could generate dangler complexes, and a Mn dangler would be most relevant as a model for the OEC. Addition of 1 equiv of Mn(OAc)₂ to a solution of **Co₄** in MeCN at 60 °C resulted in a color change from green to brown over 16 h, and in the presence of two equiv of NH₄PF₆ (to enhance solubility), a red homogeneous solution was obtained (Scheme 1). Analysis of this crude reaction mixture by HR-ESI-MS indicated the presence of a tetra(*t*-Bupy)-substituted cubane cation analogous to the previously reported [MnCo₃(μ₃-O)₄(OAc)₄(py)₄]⁺, as well as several Co^{III} acetate oligomers, most notably the dicobalt complex [Co₂(μ-OH)₂(OAc)₃(*t*-Bupy)₄]⁺ which was also identified by ¹H NMR spectroscopy (*vide infra*; Scheme 1).^{44,56} Generation of the formally Mn^{IV}Co^{III}₃ cubane corresponds to a redox reaction whereby Mn^{II} is oxidized by two equiv of Co^{III}, with one equiv of Co^{III} acting as a sacrificial oxidant (Scheme 1).

Workup of the reaction mixture involved filtration to separate the precipitated byproduct, pink Co(OAc)₂ powder (*vide infra*), followed by crystallization from CH₂Cl₂/pentane to give red crystals of [MnCo₃(μ₃-O)₄(OAc)₄(*t*-Bupy)₄][PF₆]₂ (**MnCo₃**[PF₆]₂, 47(2)% isolated yield) that were suitable for single-crystal X-ray diffraction. The solid-state molecular structure indicates retention of the basic oxo cubane framework, and the refinement improved when the metal vertex was modeled as partially occupied by Mn. Similar to what was previously observed for an analogous tetrapyrroline [MnCo₃] cubane system (with py ligands), **MnCo₃**[PF₆]₂ crystallizes as an inversion-twin in the *P* $\bar{4}$ *n*2 space group, such that ¼ of the cubane resides in the asymmetric unit, making determination of the precise location of the Mn atom impossible.⁴⁴ The ¹H

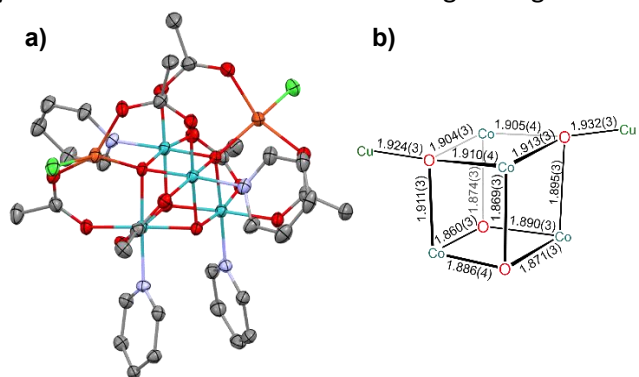
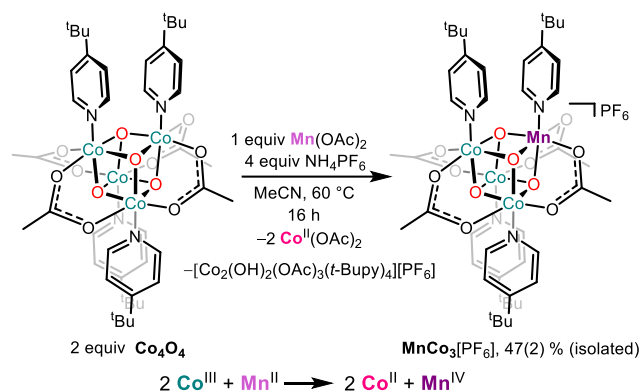


Figure 2. (a) Solid-state molecular structure of complex **Cu₂Co₄**. Solvent of recrystallization, other equiv of **Cu₂Co₄** in the asymmetric unit, and *tert*-butyl groups removed for clarity (b) Cluster bond distances.

Scheme 1. Metal-metal Exchange between Co_4 and $\text{Mn}(\text{OAc})_2$ with the Corresponding Formal Redox Equation.



NMR spectrum of $\text{MnCo}_3[\text{PF}_6]$ in acetonitrile- d_3 contained broad resonances consistent with a paramagnetic species, as confirmed by an Evans method measurement ($3.31 \mu\text{B}$, $S = 3/2$). The identity of the $[\text{Co}_2(\mu\text{-OH})_2(\text{OAc})_3(\text{t-BuPy})_4][\text{PF}_6]$ byproduct (10% yield by ^1H NMR spectroscopy) was confirmed by isolation and characterization by ^1H NMR spectroscopy and HR-ESI-MS.^{56, 57} Other Co^{III} acetate $t\text{-Bupy}$ species present (by ^1H NMR spectroscopic and mass spectrometric analysis) appear to correspond to oligomeric species.^{58, 59}

The limited solubility of $\text{Mn}(\text{OAc})_2$ in organic solvents made determination of the stoichiometry by NMR spectroscopy difficult, and motivated use of the more soluble Mn^{II} starting material $\text{Mn}(\text{OTf})_2$. Acetonitrile- d_3 solutions with various $\text{Co}_4:\text{Mn}(\text{OTf})_2$ ratios were heated to 50°C for 24 h and the reactions were

monitored by ^1H NMR spectroscopy, with 1,3,5-trimethoxybenzene (TMB) as an internal standard (Figure S94). When the $\text{Co}_4:\text{Mn}(\text{OTf})_2$ molar ratio was lower than 2:1, Co_4 was completely converted to several diamagnetic species, presumably Co^{III} oligomers (as substantiated by HR-ESI-MS), and broad paramagnetic resonances for MnCo_3^+ were observed. Consistent with the expected stoichiometry for this redox reaction, the isolated yield of $\text{MnCo}_3[\text{PF}_6]$ from the reaction of Co_4 with 1 equiv of $\text{Mn}(\text{OTf})_2$ and NH_4PF_6 was 40(5)%.

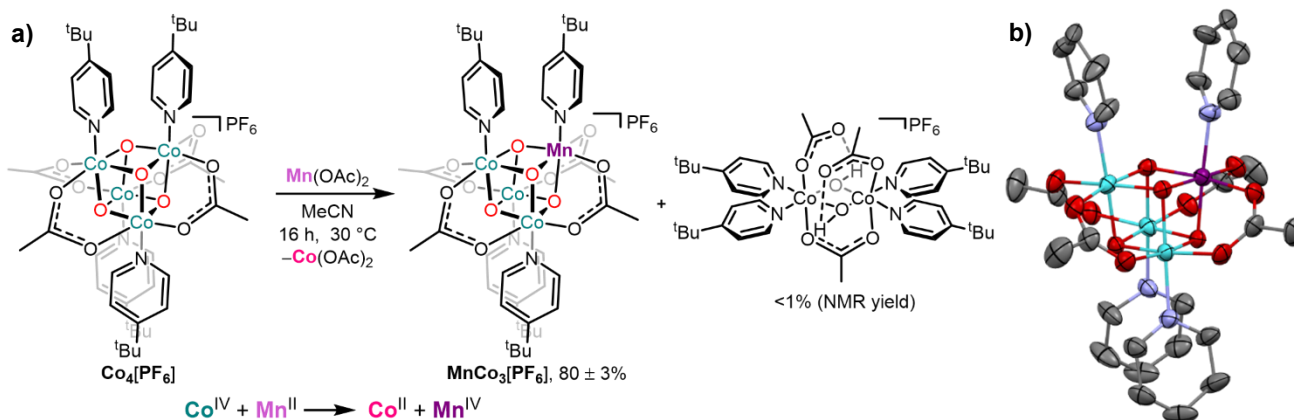


Figure 2. (a) Synthesis of $\text{MnCo}_3[\text{PF}_6]$ from $\text{Co}_4^+[\text{PF}_6]$. (b) Solid-state molecular structure of $\text{MnCo}_3[\text{PF}_6]$ with 50% probability thermal ellipsoids shown and one metal ion arbitrarily assigned as Mn (see main text). Hydrogen atoms, $t\text{-Bu}$ groups, and counterion removed for clarity.

Since the product of this metal-metal exchange reaction contains a Mn^{IV} center, the reaction of $\text{Mn}(\text{OAc})_2$ with the oxidized and formally Co^{IV} -containing $[\text{Co}^{\text{IV}}\text{Co}_3(\mu_3\text{-O})_4(\text{OAc})_4(\text{t-BuPy})_4][\text{PF}_6]$ ($\text{Co}_4^+[\text{PF}_6]$) was also examined. A vigorously stirred solution of $\text{Mn}(\text{OAc})_2$ and $\text{Co}_4^+[\text{PF}_6]$ (1:1) in MeCN at 30°C resulted in a slow color change from brown/olive green to red over 16 h (Figure 3). Removal of the solvent *in vacuo* and extraction with CH_2Cl_2 resulted in a dark brown-red solution and a pink solid (presumably $\text{Co}(\text{OAc})_2(\text{L})_n$) that was separated by filtration. Layer diffusion of pentane into the dichloromethane solution at -5°C over 48 h produced red blocks of $\text{MnCo}_3[\text{PF}_6]$ (80(3)% yield) and accordingly, HR-ESI-MS analysis of the crystalline material indicated the presence of a single cation corresponding to MnCo_3^+ . The pink solid byproduct was analyzed by HR-ESI-MS, ^1H NMR, and FTIR spectroscopy, all of which suggest the presence of $\text{Co}(\text{OAc})_2(\text{L})_n$ ($\text{L} = t\text{-Bupy}$, H_2O , Figure S110). The stoichiometry of this exchange, initiated from either $\text{Mn}(\text{OAc})_2$ or $\text{Mn}(\text{OTf})_2$ in acetonitrile- d_3 , was examined by ^1H NMR spectroscopy, and in both cases one equivalent of Mn^{II} per equivalent of Co^{IV} was required for the complete consumption of $\text{Co}_4^+[\text{PF}_6]$ (Figure S96). A trace amount (<1% yield vs internal standard) of $[\text{Co}_2(\mu\text{-OH})_2(\text{OAc})_3(\text{t-BuPy})_4][\text{PF}_6]$ in the product mixture may be attributed to reaction of residual unoxidized Co_4 in the sample of $\text{Co}_4^+[\text{PF}_6]$ (Figure S89). Monitoring the metal-metal exchange of Co_4 or $\text{Co}_4^+[\text{PF}_6]$ with $\text{Mn}(\text{OAc})_2$ by ^1H NMR spectroscopy in dry, degassed acetonitrile- d_3 in a sealed J-Young NMR tube under an N_2 atmosphere indicated that the reactions are not influenced by water and air, since the product distributions and qualitative reaction rates were unaffected. A balanced

redox equation for this metal-metal exchange reaction requires one equivalent of Co^{IV} and one equivalent of Mn^{II} to give Co^{II} and Mn^{IV} in a two-electron redox process (Figure 3)

Reactions of Co_4 with Mn^{III} sources. To probe the possible participation of intermediate Mn^{III} species in the above processes, redox reactions of Co_4 with $\text{Mn}^{\text{III}}(\text{acac})_3$ were investigated by ^1H NMR spectroscopy, with yields determined by comparison to TMB as an internal standard. An acetonitrile- d_3 solution of equimolar $\text{Mn}(\text{acac})_3$ and Co_4 , heated at 40°C for 16 h, gave complete conversion of $\text{Mn}(\text{acac})_3$, 95% conversion of Co_4 , formation of both MnCo_3^+ and $[\text{MnCo}_3(\mu_3\text{-O})_4(\text{OAc})_3(\text{acac})(t\text{-Bupy})_4]^+$ ($\text{MnCo}_3(\text{acac})^+$; by HR-ESI-MS and ^1H NMR spectroscopy), and a 27% yield of $\text{Co}(\text{acac})_3$ in addition to other unidentified paramagnetic side products. Use of two equiv of $\text{Mn}(\text{acac})_3$ led to complete conversion of Co_4 and a 92% yield of $\text{Co}(\text{acac})_3$ by ^1H NMR spectroscopy, along with the same $[\text{MnCo}_3\text{O}_4]$ cubane products according to the idealized stoichiometry outlined in Scheme 2. Note that an accurate determination of the yield and product ratios associated with MnCo_3^+ and $\text{MnCo}_3(\text{acac})^+$ is difficult to establish due to very broad ^1H NMR resonances for these paramagnetic complexes.

Presumably, one equiv of $\text{Mn}(\text{acac})_3$ is also consumed in the production of $\text{Co}(\text{acac})_3$ (Scheme 2). The $[\text{MnCo}_3\text{O}_4]$ cubane products (MnCo_3^+ and $\text{MnCo}_3(\text{acac})^+$) produced in this transformation were isolated as PF_6^- salts by chromatographic separation following the reaction of Co_4 with $\text{Mn}(\text{acac})_3$ and NH_4PF_6 which gave the coeluting products $\text{MnCo}_3[\text{PF}_6]$ and $\text{MnCo}_3(\text{acac})[\text{PF}_6]$ in a combined yield of 33%.

Another possible secondary reaction involves radical processes of the acac ligands, as this has been reported for other $\text{Mn}(\text{acac})_3$ systems.⁶⁰⁻⁶³ Indeed, a dichloromethane- d_2 solution of equimolar $\text{MnCo}_3(\mu_3\text{-O})_4(\text{OAc})_5(\text{py})_3$ and acetylacetone heated to 35°C for 16 h resulted in partial (ca. 33%) decomposition of the $[\text{MnCo}_3\text{O}_4]$ cubane and formation of $\text{Co}^{\text{III}}(\text{acac})$ products by ^1H NMR spectroscopy and HR-ESI-MS. Likewise, heating a solution containing a mixture of purified $\text{MnCo}_3[\text{PF}_6]$ and $\text{MnCo}_3(\text{acac})[\text{PF}_6]$ to 40°C resulted in depletion of $\text{MnCo}_3(\text{acac})^+$ by 25% relative to MnCo_3^+ after 16 h (HR-ESI-MS, Figure S185). Thus, radical-based reactions of acac ligands appear to contribute to a lower stability of the $\text{MnCo}_3(\text{acac})^+$ cubane and may contribute to the greater than stoichiometric consumption of Co_4 by $\text{Mn}(\text{acac})_3$ (Table 1, entries 1-3). Overall, the data in Table 1 are consistent with the stoichiometry outlined in Scheme 2.

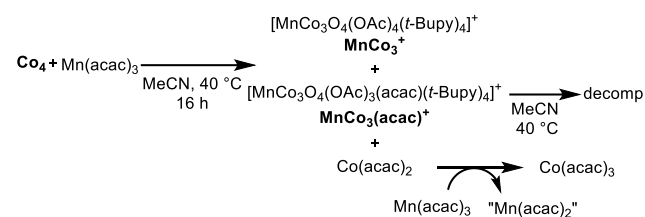
Table 1. Investigation of Mn^{III} Reagents.

[Mn] Source	Equiv	Conversion of Co_4 (%) ^a	Yield Co^{III} (%) ^a
$\text{Mn}(\text{acac})_3$	0.5	80	7
	0.75	91	11
	1	95	14
	1.5	100	29
	2	100	45
$\text{Mn}^{\text{III}}(t\text{-Bupy})[\text{PF}_6]$	0.5	44	13
	0.75	58	17
	1	69	25
	1.5	83	38
	2	100	63

^aYields determined by ^1H NMR spectroscopy vs 1,3,5-trimethoxybenzene as an internal standard as the sum of potential Co^{III} products.

resulted in quantitative conversion to $\text{Co}^{\text{III}}(t\text{-Bupy})$ by ^1H NMR spectroscopy.⁶⁴ On a synthetic scale, the reaction of two

Scheme 2. Idealized reaction of Co_4 with $\text{Mn}(\text{acac})_3$.



To limit possible side products involving acac-induced decomposition, reactions with $[\text{Mn}(\text{acac})_2(t\text{-Bupy})_2][\text{PF}_6]$ ($\text{Mn}^{\text{III}}(t\text{-Bupy})[\text{PF}_6]$), a Mn^{III} source with one less acac ligand, were also investigated. An acetonitrile- d_3 solution of equimolar $\text{Mn}^{\text{III}}(t\text{-Bupy})[\text{PF}_6]$ and Co_4 , heated at 40°C for 16 h, resulted in full conversion of $\text{Mn}^{\text{III}}(t\text{-Bupy})^+$, 69% conversion of Co_4 , a 50% yield of $[\text{Co}(\text{acac})_2(t\text{-Bupy})_2][\text{PF}_6]$ ($\text{Co}^{\text{III}}(t\text{-Bupy})[\text{PF}_6]$, Table 1) and an undetermined amount of $\text{MnCo}_3^+/\text{MnCo}_3(\text{acac})^+$ (observed by ^1H NMR and HR-ESI-MS). The reaction of Co_4 and $\text{Mn}^{\text{III}}(t\text{-Bupy})^+$ to give $\text{MnCo}_3^+/\text{MnCo}_3(\text{acac})^+$ and $\text{Co}^{\text{III}}(t\text{-Bupy})^+$ obeyed a 1:2 ($\text{Co}_4:\text{Mn}^{\text{III}}$) stoichiometry (Table 1), following a pathway analogous to that depicted in Scheme 2. Note that, unlike the reaction of Co_4 with $\text{Mn}(\text{acac})_3$, this reaction does not lead to overconsumption of Co_4 at lower $\text{Co}_4:\text{Mn}^{\text{III}}$ ratios. The conversion of Co_4 to $\text{Co}^{\text{III}}(t\text{-Bupy})^+$ suggests that one equiv of Mn^{III} undergoes metal-metal exchange with Co_4 , and another equiv of Mn^{III} oxidizes the putative $\text{Co}(\text{acac})_2$ byproduct to form one equiv of Co^{III} . In agreement with this hypothesis, the reaction of equimolar $\text{Co}(\text{acac})_2$ and $\text{Mn}^{\text{III}}(t\text{-Bupy})$ in acetonitrile- d_3

equiv of $\text{Mn}^{\text{III}}(\text{t-Bupy})[\text{PF}_6]$ with Co_4 gave an unoptimized yield of 11% for the mixture of $\text{MnCo}_3^+/\text{MnCo}_3(\text{acac})^+$, while red crystals of $\text{Co}^{\text{III}}(\text{t-Bupy})[\text{PF}_6]$ were isolated in 42% yield.

By ^1H NMR spectroscopy, no reaction occurred for an acetonitrile- d_3 solution of $\text{MnCo}_3(\mu_3\text{-O})_4(\text{OAc})_5(\text{py})_3$ and $[\text{Mn}(\text{acac})_2(\text{py})_2][\text{PF}_6]$ ($\text{Mn}^{\text{III}}(\text{py})[\text{PF}_6]$) heated to 40°C for 16 h. This indicates that a secondary reaction of the $[\text{MnCo}_3\text{O}_4]$ cubane product with $\text{Mn}^{\text{III}}(\text{py})^+$ does not influence the observed product distributions under these conditions. Additionally, monitoring the reaction of Co_4 with $\text{Mn}^{\text{III}}(\text{t-Bupy})^+$ by ^1H NMR spectroscopy indicates that a non-oxidative ligand exchange does not compete with metal-metal exchange for the consumption of Co_4 in the reaction of Co_4 and $\text{Mn}^{\text{III}}(\text{t-Bupy})^+$. Thus, the Co-Mn exchange involving Co_4 and $\text{Mn}^{\text{III}}(\text{t-Bupy})^+$ more closely follows the idealized stoichiometry of Scheme 2 and early in this reaction there are no significant, competing processes that consume Co_4 . The reduced 63% yield of Co^{III} in the 1:2 reaction of Co_4 with $\text{Mn}^{\text{III}}(\text{t-Bupy})^+$ is likely due to radical-induced processes.

Metal-Metal Exchange Kinetics Involving Mn^{III} . To probe the mechanism of cobalt-manganese exchange, kinetic studies involving $[\text{Co}_4\text{O}_4]$ cubanes and Mn^{III} complexes were conducted, using initial rate data collected from reactions monitored by UV-vis spectroscopy. The cobalt oxo cubanes chosen for study are benzoate derivatives that allow tuning of the cubane electronic properties with *para* substituents in the pyridine and benzoate ligands. These substituted pyridine and benzoate complexes, e.g., $\text{Co}_4(\mu_3\text{-O})_4(\text{OBz})_4(\text{py})_4$ ($\text{Co}_4(\text{py-H})$) and $\text{Co}_4(\mu_3\text{-O})_4(\text{OBz})_4(\text{t-Bupy})_4$ ($\text{Co}_4(\text{O}_2\text{CC}_6\text{H}_4\text{-H})$), were readily prepared by the known procedure involving $\text{Co}(\text{OAc})_2(\text{H}_2\text{O})_4$ and the corresponding pyridine with H_2O_2 , or by ligand-exchange reactions of a benzoic acid derivative with Co_4 (see SI).⁶⁵⁻⁶⁷ The Mn^{III} -based reactant $[\text{Mn}(\text{acac})_2(\text{py})_2][\text{PF}_6]$ $\text{Mn}^{\text{III}}(\text{py})[\text{PF}_6]$ was chosen due to its favorable solubility properties and slow rates of ligand-exchange side reactions. As determined by ^1H NMR spectroscopy, no reaction was observed within 0.5 h of combining equimolar solutions of $\text{Mn}^{\text{III}}(\text{py})^+$ and $\text{Co}_4(\text{py-H})$. The Mn-Co exchange proceeds in a manner similar to that involving Co_4 and $\text{Mn}^{\text{III}}(\text{t-Bupy})^+$, to give $[\text{MnCo}_3(\mu_3\text{-O})_4(\text{OBz})_4(\text{py})_4][\text{PF}_6]$ ($\text{MnCo}_3(\text{py})[\text{PF}_6]$) and $[\text{Co}(\text{acac})_2(\text{py})_2][\text{PF}_6]$ ($\text{Co}^{\text{III}}(\text{py})[\text{PF}_6]$). Critically, there are no side reactions that occur before metal-metal exchange in the reaction with Mn^{III} sources and $\text{Co}_4(\text{py-H})$, and it is assumed that the measured initial rates are minimally affected by competing secondary processes. Note that ligand exchange was observed in other cases; for example, $\text{Mn}(\text{OTf})_2$ reacts rapidly with Co_4 by initial ligand exchange, to give triflate-containing cobalt cubane complexes (by ^1H NMR and ESI-MS; Figure S99) before metal-metal exchange occurred. Ligand exchange was also observed in the transfer of an acac ligand in the reaction of Co_4 with $\text{Mn}(\text{acac})_3$ (eq 2), which suggests operation of an inner-sphere electron-transfer process.

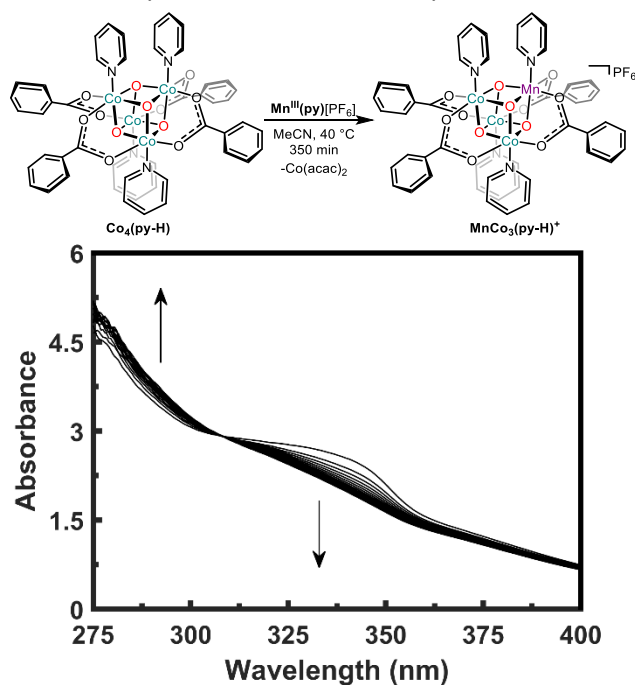


Figure 3. Representative UV-vis spectra tracking the metal-metal exchange reaction between equimolar $\text{Mn}^{\text{III}}(\text{py})^+$ and $\text{Co}_4(\text{py-H})$ over 350 min.

Equimolar MeCN solutions of $\text{Co}_4(\text{py-H})$ and $\text{Mn}^{\text{III}}(\text{py})^+$ were combined in a sealed cuvette and the resulting reaction mixture was heated to 40°C for 350 minutes. Monitoring by UV-vis spectroscopy revealed an approximate isosbestic point at 308 nm (Figure 3), indicating a linear relationship between the concentrations of products and reactants. Generally, in further kinetics experiments, the entire UV-vis spectrum was collected at each timepoint, and rate data was determined simultaneously in triplicate to estimate the experimental error. Attempts to fit the data to an integrated rate law did not cleanly delineate between various mechanistic possibilities, likely due to the aforementioned background oxidation reaction of $\text{Co}(\text{acac})_2$ to give $\text{Co}^{\text{III}}(\text{py})$.

Kinetics for the metal-metal exchange reaction were followed by UV-vis spectroscopy, with an excess of $\text{Co}_4(\text{py-H})$ or $\text{Mn}^{\text{III}}(\text{py})^+$ to establish pseudo first-order conditions. The slope of the log/log plot of $[\text{Mn}^{\text{III}}(\text{py})^+]_0$ vs. k_{init} (Figure 5) indicated a reaction order of 0.8(2), while the log/log plot of $[\text{Co}_4(\text{py-H})]_0$ vs. k_{init} indicated a reaction order of 0.55(3) (Figure S143). Although the fractional reaction orders are difficult to interpret, the dependence of the rate on both $\text{Mn}^{\text{III}}(\text{py})^+$ and $\text{Co}_4(\text{py-H})$ concentrations indicates that both species are involved in a rate-determining step. This behavior is consistent with both outer- and inner-sphere electron-

transfer mechanisms, but an inner-sphere redox process in an intermediate adduct formed by coordination of $\text{Mn}^{\text{III}}(\text{py})^+$ to a μ_3 -oxo ligand of $\text{Co}_4(\text{py-H})$ seems likely. Note that in the observations described above, ligand transfer often, but not always, accompanies metal-metal exchange (*vide supra*).

Given the apparent lability of the complexes in this process, the role of added ligands on the reaction kinetics was investigated by monitoring the reaction of $\text{Co}_4(\text{py-H})$ and $\text{Mn}^{\text{III}}(\text{py})^+$ in the presence of added pyridine or benzoate (as $^n\text{Bu}_4\text{NOBz}$). Additional pyridine had no discernible effect on k_{init} (Figure S145), indicating that pyridine ligand dissociation does not significantly influence the rate of metal-metal exchange. Additional benzoate inhibited the rate of metal-metal exchange, as indicated by the $-1.0(3)$ order dependence of k_{init} on $[\text{Bu}_4\text{NOBz}]_0$; this inhibitory effect could result from binding of benzoate to $\text{Mn}^{\text{III}}(\text{py})^+$ to render it less reactive. Alternatively, benzoate might add to the cubane via coordination to a cobalt center, to form an anionic complex. While a solution of $^n\text{Bu}_4\text{NOBz}$ and Co_4 (1:1) remained unchanged after 16 h (by ^1H NMR spectroscopy), addition of $^n\text{Bu}_4\text{NOBz}$ (1 equiv) to a solution of $\text{Mn}^{\text{III}}(\text{py})^+$ in acetonitrile- d_3 immediately resulted in several new products, as indicated by broad resonances in the ^1H NMR spectrum. It is presumed that benzoate adds to $\text{Mn}^{\text{III}}(\text{py})^+$ to generate one or more less-reactive (likely less electrophilic) Mn complexes. The rate of metal-metal exchange was also examined in CH_2Cl_2 , *ortho*-difluorobenzene, DMSO, 1,1,2,2-tetrachloroethane, and THF; however, no relationship between the solvent dielectric constant and k_{init} was discerned across this series.

The above results are consistent with the simplified mechanistic model for metal-metal exchange shown in Scheme 3. Initially, the $[\text{Co}_4\text{O}_4]$ cubane binds the incoming Mn center by donation from a μ_3 -oxo ligand, which is likely assisted by an acetate migration (A). An inner-sphere electron transfer in this intermediate produces a Co^{II} center, which should significantly weaken the resulting $\mu_4\text{-O}-\text{Co}^{\text{II}}$ bond (B). Note that $\text{Co}-\text{O}$ bond elongations occur upon binding a Lewis acid, even without a reduction process as observed in dicopper adduct Cu_2Co_4 (*vide supra*), but $\text{Co}-\text{O}$ bond elongations are expected to be more pronounced with a reduced Co^{II} center and the resulting population of $\text{Co}-\text{O}$ antibonding orbitals. The more labile Co^{II} center should then readily participate in a reorganization that exchanges it for the Mn^{IV} ion that is more stable in the octahedral site of the cubane (C). Note that this rearrangement may occur without dissociation or change in the binding mode for the acetate ligands, to give a MnCo_3 oxo cubane core with a labile Co^{II} species in a “dangler” position, analogous to that of the previously isolated complex $\text{MnCo}_4(\mu_4\text{-O})(\mu_3\text{-O})_3(\text{OAc})_6(\text{NO}_3)(\text{py})_3$.⁴⁶ This labile Co^{II} ion is readily lost by ligand exchange reactions in the reaction mixture; however, this step may be relatively slow given isolation of the aforementioned nitrate analogue. Evidence for an analogous dangler intermediate during metal-metal exchange comes from ^1H NMR monitoring of the formation of MnCo_3 from the reaction of Co_4 and $\text{Mn}(\text{OAc})_2$, which reveals the build-up of an intermediate, proposed to be $\text{MnCo}_4(\mu_4\text{-O})(\mu_3\text{-O})_3(\text{OAc})_7(t\text{-Bupy})_3$, with resonances corresponding to those for $\text{MnCo}_4(\mu_4\text{-O})(\mu_3\text{-O})_3(\text{OAc})_6(\text{NO}_3)(\text{py})_3$ (Figure S98). In general, the binding of a Lewis acidic metal center to a bridging oxo ligand is expected to raise the reduction potential of the cubane. As described above, this effect is observed in complex Cu_2Co_4 , and is also observed for the protonated cobalt oxo cubane, which exhibits an irreversible reduction at approximately -0.6 V vs. Fc/Fc^+ in MeCN.⁶⁷ It is noteworthy that Mn^{III} reduces Co^{II} in this scenario because Mn^{III} complexes such as $\text{Mn}(\text{acac})_3$ ($\text{Mn}^{\text{III/IV}}$ $E_{1/2}$ in MeCN = 0.58 V vs. Fc/Fc^+), $\text{Mn}^{\text{III}}(t\text{-Bupy})^+$, and basic manganese acetate $\text{Mn}_3(\text{OAc})_6(\text{H}_2\text{O})_3(\mu_3\text{-O})$, are generally mild oxidants that would not be expected to reduce Co_4 (E_{pc} in MeCN = ~ -1.3 V vs. Fc/Fc^+) in an outer sphere manner.⁶⁸⁻⁷⁰

In general, the binding of a Lewis acidic metal center to a bridging oxo ligand is expected to raise the reduction potential of the cubane. As described above, this effect is observed in complex Cu_2Co_4 , and is also observed for the protonated cobalt oxo cubane, which exhibits an irreversible reduction event at approximately -0.6 V vs. Fc/Fc^+ in MeCN.⁶⁷ It is noteworthy that Mn^{III} reduces Co^{II} in this scenario because Mn^{III} complexes such as $\text{Mn}(\text{acac})_3$ ($\text{Mn}^{\text{III/IV}}$ $E_{1/2}$ in MeCN = 0.58

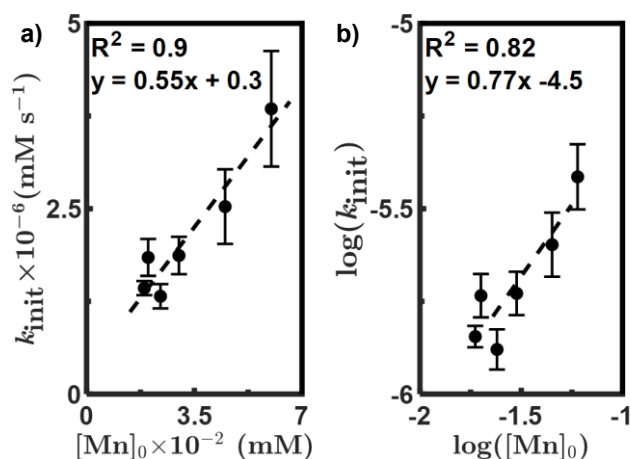
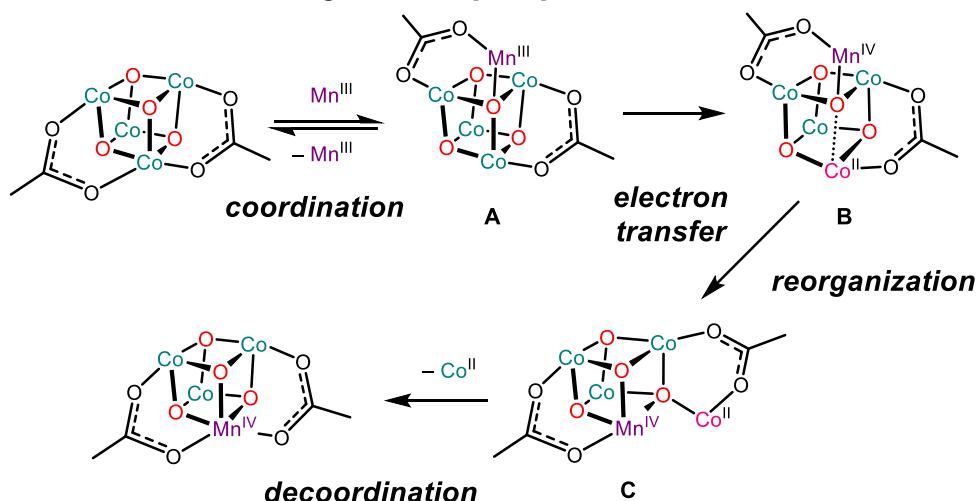


Figure 4. Linear Relationship between $[\text{Mn}^{\text{III}}(\text{py})^+]_0$ and the initial rate constant for metal-metal exchange between $\text{Co}_4(\text{py-H})$ and $\text{Mn}^{\text{III}}(\text{py})^+$. (a) $[\text{Mn}^{\text{III}}(\text{py})^+]_0$ vs the rate of metal-metal exchange; k_{init} varies linearly with $[\text{Mn}^{\text{III}}(\text{py})^+]_0$. (b) Double logarithm plot of $[\text{Mn}^{\text{III}}(\text{py})^+]_0$ vs. k_{init} indicating a reaction order of 0.8(2) order in $[\text{Mn}^{\text{III}}(\text{py})^+]_0$.

Scheme 3. Proposed Mechanism for M-M Exchange Between a [Co₄O₄] Cubane and Mn^{III}.



V vs. Fc/Fc⁺), **Mn^{III}(t-Bupy)⁺**, and basic manganese acetate Mn₃(OAc)₆(H₂O)₃(μ₃-O), are generally mild oxidants that would not be expected to reduce Co₄ (*E*_{pc} in MeCN = ~-1.3 V vs. Fc/Fc⁺) in an outer sphere manner.⁶⁸⁻⁷⁰ This mismatch in redox potentials between Mn^{III} sources and Co₄O₄ cubanes supports the hypothesis that an outer-sphere electron transfer pathway for metal-metal exchange is unlikely. Thus, the structural data of Cu₂Co₄ and electrochemical data of Co₄, Cu₂Co₄, and Mn^{III}(py), support the hypothesis that the reduction from Co^{III} to Co^I occurs in an intermediate pentametalllic species such as **A**.

The reduction of a substitutionally inert, low spin, d⁶ Co^{III} ion by a d⁴ Mn^{III} ion is reminiscent of the classic studies on inner-sphere electron transfer between Co^{III}Cl and a d⁴ Cr^{II} ion, to give Co^{II} and Cr^{III}Cl.^{71,72} However, in the Co-Mn exchanges discussed here, ligand exchange is likely a consequence of the binding event (**A**) and the dynamic behavior of the acetate ligands, rather than electron transfer through an acetate bridge.⁷³ In this inner-sphere process, the bridging ligand critical to electron-transfer is probably the μ₄-oxo ligand.⁷⁴⁻⁷⁶ Nonetheless, the carboxylate ligands are assumed to play an important, secondary role in influencing the electron-transfer driving force by modulating redox potentials, and by contributing to the rate of initial adduct formation.

To investigate these electronic effects on the reaction rates, Hammett plots were constructed with data from reactions of cubanes possessing substituted pyridine and benzoate ligands. Due to solubility constraints, the data were collected on reactions in CH₂Cl₂, with 10 equiv of Mn^{III}(py) or Mn^{III}(t-Bupy) to give pseudo first-order conditions. Interestingly, a plot of *k*_{init} vs. σ_{para} parameters shows that for benzoate ligands, the rate may be accelerated by both electron-donating and electron-withdrawing substituents (Figure 5), suggesting the operation of opposing electronic effects. More donating benzoate ligands (X = tBu, Me) are expected to promote the basicity of the μ₃-oxo ligands, thereby favoring formation of adduct species **A**. On the other hand, electron-withdrawing substituents (X = NO₂, CN, Br, Cl) decrease the basicity of the oxo ligands, but increase the reduction potential of the cubane, rendering Co^{III} more susceptible to the reduction step to produce **C**. An inflection point associated with the balance between these two effects corresponds to X = H/Ph.

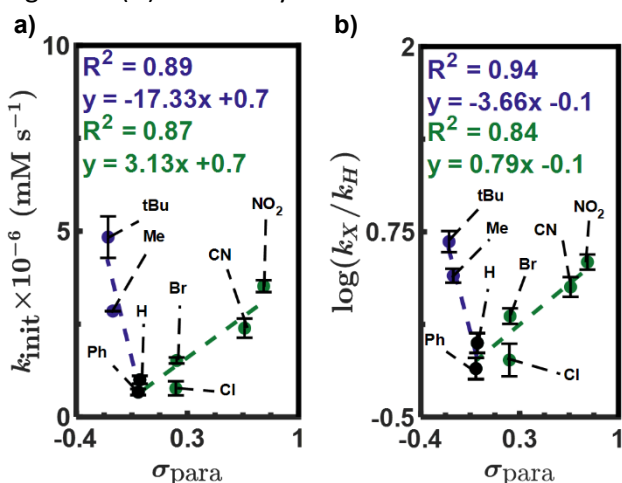


Figure 5. Influence of the *para*-benzoate ligand substituent of Co₄(O₂CC₆H₄-X) on the initial rate constant for metal-metal exchange. (a) *para*-Hammett parameter vs. initial rate constant of metal-metal exchange for Co₄(O₂CC₆H₄-tBu, -Me, -Ph, -H, -Cl, -Br, -CN, and -NO₂). Rates increase with both more donating (tBu, Me, H) and withdrawing (NO₂, CN, Cl, Br, H) substituents, with an inflection point at Co₄(O₂CC₆H₄-H). (b) Hammett plot relating the *para*-benzoate substituent and log(*k*_x/*k*_H) with ρ values determined from the slope of the linear fits. The ρ value for electron donating substituents (-3.7(6)) compared to ρ for the electron withdrawing substituents (0.8(2)) indicates that benzoate plays a more substantial role in the electron donating regime than it does in the electron withdrawing regime.

The influence of the more basic benzoate ligands, determined by the ratio of the rate constants k_X/k_H ($\rho = -3.7(6)$), is greater than that of the more acidic benzoate ligands ($\rho = 0.8(2)$), which indicates that the ability of the cubane to coordinate Mn^{III} is critical to metal-metal exchange reactivity. This would suggest that for the Co_4O_4 cubane system, the Lewis acidity of the incoming metal ion is more important than its reducing potential in influencing the rate of metal-metal exchange. Interestingly, the most electron-rich oxo cubane in this series, $Co_4(O_2CC_6H_4-OMe)$, reacts with $Mn^{III}(t-Bupy)^+$ but does not undergo metal-metal exchange (by 1H NMR spectroscopy). This is perhaps due to stabilization of the oxidized cubane, $Co_4(O_2CC_6H_4-OMe)^+$ in this case.

In the case of the substituted pyridine ligands, stronger donors result in faster metal-metal exchange, and the small, negative slope ($\rho = -0.4(1)$) from the Hammett plot indicates that pyridine substituents are less effective than benzoates in modulating k_{init} (Figure 6). This is consistent with previous observations that the pyridine ligands impact the redox properties less than the chelating, anionic ligands.⁶⁶

Role of Acetate and Pyridine Ligand Transfers in Co-Mn Exchange. To further investigate the role of ligand transfer during metal-metal exchange, deuterium-labeling studies were conducted on acetate complexes. When an MeCN solution of Co_4 was treated with the Mn^{II} reagent $Mn(OAc-d_3)_2$ (corresponding to a 4-fold excess of $OAc-d_3$) for 48 h at only 23 °C, HR-ESI-MS analysis did not detect $MnCo_3^+$ as a product, while complete scrambling of the $OAc-d_3$ label into Co_4 gave a binomial distribution of isotopologues (Figure S197). This indicates that the initial adduct formation step in the metal-metal exchange process to give **A** may be reversible. Heating an identical reaction mixture at 70 °C for 2 h, and analysis by HR-ESI-MS, revealed that acetate ligand scrambling was incomplete as judged by the degree of $OAc-d_3$ incorporation into Co_4 (33%) and $MnCo_3^+$ (51%). Thus, acetate ligand exchange appears to be somewhat faster than metal-metal exchange such that the latter is accompanied by some degree of acetate ligand transfer. In another set of experiments, an acetonitrile solution of oxidized cubane $Co_4^+[PF_6]$ was treated with 2 equiv of $Mn(OAc-d_3)_2$ at 40 °C for 2 h. In this case, HR-ESI-MS analysis revealed 39% incorporation of the acetate label compared to 30% incorporation of the label in “unreacted” Co_4^+ . These experiments indicate that the cubane acetate ligands can exchange with the Mn acetate ligands before and during the metal-metal exchange reaction and suggests that a pentametallic complex may form during the metal-metal exchange process. In both cases, a binomial distribution of labeled acetates was also observed for the byproducts $Co(OAc)_n(OAc-d_3)_{2-n}$ ($n = 0-2$) and $[Co_2(\mu_2-OH)_2(OAc)_n(OAc-d_3)_{3-n}(t-Bupy)_4]^+$ ($n = 0-3$).

For comparison, acetate ligand incorporation into cubane Co_4 from acetic acid and acetate was examined. A MeCN solution of Co_4 was stirred with four equiv of acetic acid- d_4 , or triethylammonium acetate- d_4 (generated in situ by treatment of triethylamine with acetic acid- d_4) at 23 °C, and the reaction mixtures were subjected to HR-ESI-MS analysis. In both experiments, the deuterium label was incorporated rapidly (ca. 10 min), resulting in a binomial distribution of all five possible cubane isotopologues $Co_4(\mu_3-O)_4(OAc)_n(OAc-d_3)_{4-n}$ ($n = 0-4$). In a control experiment, equimolar MeCN solutions of $Co_4(\mu_3-O)_4(OAc)_4(py)_4$ and $Co_4(\mu_3-O)_4(OAc-d_3)_4(py-d_5)_4$ (the fully deuterated isotopologue) were combined and after 24 h at 40 °C, no acetate or pyridine isotope crossover was observed by HR-ESI-MS, which is consistent with slow ligand dissociation from a low spin Co^{III} center (Figure S192). In the presence of 2 equiv of $Mn(OAc)_2$, and heating at 70 °C for 0.5 h, these isotopologues undergo exchange of pyridine ligands. Analysis by HR-ESI-MS revealed a binomial distribution of all possible product isotopologues of the starting cubane $Co_4(\mu_3-O)_4(OAc)_4(py)_n(py-d_5)_{4-n}$ ($n = 1-4$) before any of the corresponding Mn cubane was detected. This experiment indicates that the pyridine ligands redistribute before the metal-metal exchange reaction. It should be noted that a redistribution of pyridine ligands was also observed when HOAc was

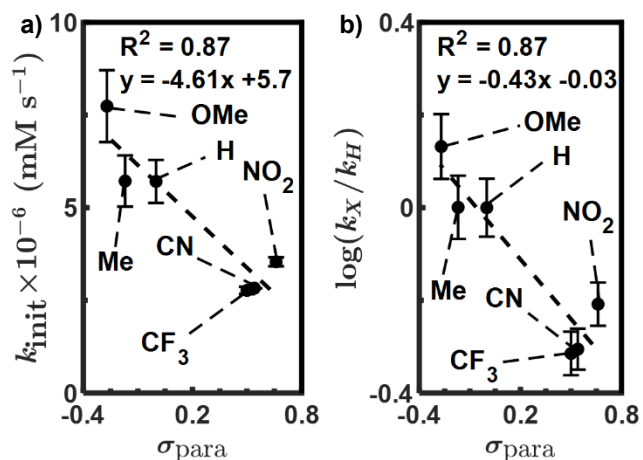


Figure 6. Influence of *para*-pyridyl substituents of $Co_4(py-X)$ on the rate constant for metal-metal exchange. (a) *para*-Hammett parameter vs. initial rate of metal-metal exchange for $Co_4(py-OMe, -Me, -H, -CF_3, -CN, -NO_2)$. The rate inversely correlates with the Hammett parameter (σ_{para}) of the substituent, with stronger donors leading to more rapid exchange. (b) Hammett plot relating the *para*-pyridyl substituent and $\log(k_X/k_H)$ with ρ determined from the slope of the linear fit. The low ρ value ($-0.4(1)$) determined from the Hammett plot is consistent with prior observations that the pyridine ligands influence the cubane redox potentials less than the chelating ligands (S140), with the pyridine ligands mostly tuning the basicity of the oxo ligands.

added in place of $\text{Mn}(\text{OAc})_2$ under otherwise identical conditions. A pyridine-exchange process involving related dinuclear cobalt species has been reported.⁵⁶

In summary, the acetate ligands of a $[\text{Co}_4\text{O}_4]$ cubane exchange with the acetate ligands of $\text{Mn}(\text{OAc}-d_3)_2$, and this process is competitive with metal-metal exchange. The $[\text{Co}_4\text{O}_4]$ cubane pyridine ligands exchange under the experimental conditions at a rate significantly faster than metal-metal exchange, which indicates a pyridine-dissociative mechanism, but the measured order in pyridine indicates that this does not influence the metal-metal exchange reactivity. The observed isotopologues of MnCo_3^+ produced in these labeling experiments suggest the formation of an intermediate pendent metal complex in which ligand exchange is facile.

Concluding Remarks

The study described here significantly enhances the small but growing knowledge base associated with the synthesis and properties of transition metal oxo cubanes that possess an associated “dangler” metal ion. Such clusters may serve as models for the $\text{Mn}[\text{CaMn}_3\text{O}_4]$ oxygen evolving complex, especially if the dangler ion is redox active and bound to the cubane through carboxylate bridges.^{19,20,45} Formation of the dicopper dangler Cu_2Co_4 from well-defined precursors, by use of additional acetate ligands to tether the copper ions to the cubane, provides a unique example whereby dangler ions are bound to a $[\text{Co}_4\text{O}_4]$ cubane. Notably, the acetate ligands in this complex, like the carboxylate groups of the OEC, support a dangler ion- μ_4 -oxo interaction that may play an important role in chemical transformations of the assembly. In the OEC, the comparable dangler interaction is thought to enable the structural changes required for water activation.³⁷ Indeed, attempts to extend the synthesis of Cu_2Co_4 to manganese provides evidence for formation of a carboxylate-supported $\text{Mn}[\text{Co}_4\text{O}_4]$ intermediate complex possessing a $\text{Mn}(\mu_4\text{-O})\text{Co}_3$ arrangement. The latter transitory structure appears to be key to electron-transfer processes that ultimately lead to a redox-driven exchange of metals that introduce manganese *via* a structural rearrangement of the oxo cubane core.

These studies on the chemical behavior of metal clusters in solution provide design principles for the development of new metal-metal exchange reactions.²⁵ The observed exchange reaction is a rare example of a well-defined metal-metal redox exchange for a tetrametallic cubane cluster. Importantly, the efficiency of this process suggests its broader utility for the controlled synthesis of predetermined oxo metal clusters with intricate structures.⁷⁷ Furthermore, the conveyance of a manganese ion to a cubane cluster is perhaps relevant to the biochemical mechanism for assembly of the OEC, which is believed to occur by photochemically driven redox processes whereby Mn^{II} is incorporated by a stepwise process into the cluster.^{31,78} Additionally, the details of metal additions and exchanges of this sort may help in the development of synthetic schemes for assembly of mixed-metal nanoclusters and bulk materials. Indeed, related galvanic exchange reactions have been employed to modify an oxide or sulfide structure to incorporate a heterometal.^{51-53,77,79}

Further investigations into the role of redox active dangler ions should help shed light on the possible role of these species in controlling chemical transformations of the oxo cluster core. The concepts developed in this study are now being used in syntheses of heterometallic oxo cubanes.

Associated Content

Experimental details, characterization data, kinetics data and crystallographic details. Accession Codes 2349139-2349140 (Cu_2Co_4) and ($[\text{MnCo}_3][\text{PF}_6]$) contain the supplementary crystallographic data for this paper. These data can be obtained free of charge through www.ccdc.ac.uk/data_request/cif or by emailing data_request@ccdc.cam.ac.uk, or by contacting The Cambridge Crystallographic Data Centre, 12 Union Road, Cambridge CB2 1EZ, UK; fax: +44 1223 336033.

Author Information

Corresponding Author

T. Don Tilley – *Department of Chemistry, University of California, Berkeley, Berkeley, California 94720, United States; Chemical Sciences Division, Lawrence Berkeley National Laboratory, Berkeley, California 94720, United States;*

Author

T. Alex Wheeler – *Department of Chemistry, University of California, Berkeley, Berkeley, California 94720, United States; Chemical Sciences Division, Lawrence Berkeley National Laboratory, Berkeley, California 94720, United States;*

Acknowledgments

This work was funded by the U.S. Department of Energy, Office of Science, Office of Basic Energy Sciences, Chemical Sciences, Geosciences, and Biosciences Division, under Contract DE-AC02-05CH11231. The LBNL Catalysis Laboratory provided HR-ESI-MS, FTIR, and UV-vis instrumentation. This research used the resources of the Advanced Light Sources, which is a DOE Office of Sciences User Facility under contract no. DE-AC02-05CH11231. NMR spectra were collected at the College of Chemistry Pines Magnetic Resonance Center's Core NMR Facility, at the University of California, Berkeley, which is supported in part by the National Institutes of Health under grant no. S10Od024998. The authors thank Drs. Hasan Celik, Alicia Lund, and Raynald Giovine, for assistance with NMR spectroscopy, Dr. Simon Teat for assistance with crystallography, and Drs. Cooper Citek, Chithra Asokan, and Miao Zhang for assistance with LBNL Catalysis Laboratory instrumentation. Dr. Rex Handford, Dr. Benjamin Suslick, Dr. Jaruwat Amtawong, Dr. Stefan Künzi, and Matt See are thanked for their thoughtful discussion and consideration of this manuscript.

References:

- (1) Huang, H. L.; Brudvig, G. W. Oxygen Evolution of Photosystem II. In *Comprehensive Coordination Chemistry III*; Elsevier, 2021; Chapter 22, pp 569-588.
- (2) Yano, J.; Yachandra, V., Mn₄Ca Cluster in Photosynthesis: Where and How Water is Oxidized to Dioxygen. *Chem. Rev.* **2014**, *114*, 4175-4205.
- (3) Beinert, H., Iron-Sulfur Proteins: Ancient Structures, Still Full of Surprises. *J. Biol. Inorg. Chem.* **2000**, *5*, 2-15.
- (4) Bigness, A.; Vaddypally, S.; Zdilla, M. J.; Mendoza-Cortes, J. L., Ubiquity of Cubanes in Bioinorganic Relevant Compounds. *Coord. Chem. Rev.* **2022**, *450*.
- (5) Brown, A. C.; Suess, D. L. M. Synthetic Iron-Sulfur Clusters. In *Comprehensive Coordination Chemistry III*, Elsevier, 2021; Chapter 8 pp 134-156.
- (6) Johnson, D. C.; Dean, D. R.; Smith, A. D.; Johnson, M. K., Structure, Function, and Formation of Biological Iron-Sulfur Clusters. *Annu. Rev. Biochem.* **2005**, *74*, 247-81.
- (7) Liu, J.; Chakraborty, S.; Hosseinzadeh, P.; Yu, Y.; Tian, S.; Petrik, I.; Bhagi, A.; Lu, Y., Metalloproteins Containing Cytochrome, Iron-Sulfur, or Copper Redox Centers. *Chem. Rev.* **2014**, *114*, 4366-4469.
- (8) Barber, J., A Mechanism for Water Splitting and Oxygen Production in Photosynthesis. *Nat. Plants* **2017**, *3*, 17041.
- (9) Lee, S. C.; Lo, W.; Holm, R. H., Developments in the Biomimetic Chemistry of Cubane-Type and Higher Nuclearity Iron-Sulfur Clusters. *Chem. Rev.* **2014**, *114*, 3579-3600.
- (10) Paul, S.; Neese, F.; Pantazis, D. A., Structural Models of the Biological Oxygen-Evolving Complex: Achievements, Insights, and Challenges for Biomimicry. *Green Chemistry* **2017**, *19*, 2309-2325.
- (11) Wieghardt, K., The Active Sites in Manganese-Containing Metalloproteins and Inorganic Model Complexes. *Angew. Chem. Int. Ed.* **1989**, *28*, 1153-1172.
- (12) Dismukes, G. C.; Brimblecombe, R.; Felton, G. A. N.; Pryadun, R. S.; Sheats, J. E.; Spiccia, L.; Swiegers, G. F., Development of Bioinspired Mn₄O₄-Cubane Water Oxidation Catalysts: Lessons from Photosynthesis. *Acc. Chem. Res.* **2009**, *42*, 1935-1943.
- (13) Brudvig, G. W.; Thorp, H. H.; Crabtree, R. H., Probing the Mechanism of Water Oxidation in Photosystem II. *Acc. Chem. Res.* **1991**, *24*, 311-316.
- (14) Christou, G., Manganese Carboxylate Chemistry and Its Biological Relevance. *Acc. Chem. Res.* **1989**, *22*, 328-335.
- (15) Lee, H. B.; Tsui, E. Y.; Agapie, T., A CaMn₄O₂ Model of the Biological Oxygen Evolving Complex: Synthesis via Cluster Expansion on a Low Symmetry Ligand. *Chem. Commun.* **2017**, *53*, 6832-6835.
- (16) Lee, H. B.; Marchiori, D. A.; Chatterjee, R.; Oyala, P. H.; Yano, J.; Britt, R. D.; Agapie, T., S = 3 Ground State for a Tetranuclear Mn^{IV}₄O₄ Complex Mimicking the S₃ State of the Oxygen-Evolving Complex. *J. Am. Chem. Soc.* **2020**, *142*, 3753-3761.
- (17) Yachandra, V. K.; Sauer, K.; Klein, M. P., Manganese Cluster in Photosynthesis: Where Plants Oxidize Water to Dioxygen. *Chem. Rev.* **1996**, *96*, 2927-2950.

- (18) Lee, H. B.; Shiau, A. A.; Marchiori, D. A.; Oyala, P. H.; Yoo, B.-K.; Kaiser, J. T.; Rees, D. C.; Britt, R. D.; Agapie, T., CaMn_3VO_4 Cubane Models of the Oxygen-Evolving Complex: Spin Ground States $S < 9/2$ and the Effect of Oxo Protonation. *Angew. Chem. Int. Ed.* **2021**, *60*, 17671-17679.
- (19) Kanady, J. S.; Lin, P.-H.; Carsch, K. M.; Nielsen, R. J.; Takase, M. K.; Goddard, W. A.; Agapie, T., Toward Models for the Full Oxygen-Evolving Complex of Photosystem II by Ligand Coordination To Lower the Symmetry of the Mn_3CaO_4 Cubane: Demonstration That Electronic Effects Facilitate Binding of a Fifth Metal. *J. Am. Chem. Soc.* **2014**, *136*, 14373-14376.
- (20) Zhang, C.; Chen, C.; Dong, H.; Shen, J.-R.; Dau, H.; Zhao, J., A Synthetic Mn_4Ca -Cluster Mimicking the Oxygen-Evolving Center of Photosynthesis. *Science* **2015**, *348*, 690-693.
- (21) Lee, H. B.; Oyala, P. H.; Agapie, T., Synthesis, Electronic Structure, and Spectroscopy of Multinuclear Mn Complexes Relevant to the Oxygen Evolving Complex of Photosystem II. In *Oxygen Production and Reduction in Artificial and Natural Systems*, Wolrd Scientific: 2018; pp 259-283.
- (22) Shiau, A. A.; Lee, H. B.; Oyala, P. H.; Agapie, T., Coordination Number in High-Spin–Low-Spin Equilibrium in Cluster Models of the S_2 State of the Oxygen Evolving Complex. *J. Am. Chem. Soc.* **2023**, *145*, 14592-14598.
- (23) Chen, C.; Chen, Y.; Yao, R.; Li, Y.; Zhang, C., Artificial Mn_4Ca Clusters with Exchangeable Solvent Molecules Mimicking the Oxygen-Evolving Center in Photosynthesis. *Angew. Chem., Int. Ed.* **2019**, *58*, 3939-3942.
- (24) Chen, Q.-F.; Guo, Y.-H.; Yu, Y.-H.; Zhang, M.-T., Bioinspired Molecular Clusters for Water Oxidation. *Coord. Chem. Rev.* **2021**, *448*, 214164.
- (25) Thompson, N. B.; Namkoong, G.; Skeel, B. A.; Suess, D. L. M., Facile and Dynamic Cleavage of Every Iron–Sulfide Bond in Cuboidal Iron–Sulfur Clusters. *Proc. Natl. Acad. Sci. U.S.A.* **2023**, *120*, e2210528120.
- (26) Hong, J. S.; Rabinowitz, J. C., Base-catalyzed Exchange of the Iron and Sulfide of Clostridial Ferredoxin. *J. Biol. Chem.* **1970**, *245*, 6582-6587.
- (27) Britt, R. D.; Rao, G.; Tao, L., Bioassembly of Complex Iron–Sulfur Enzymes: Hydrogenases and Nitrogenases. *Nat. Rev. Chem.* **2020**, *4*, 542-549.
- (28) Badding, E. D.; Srisantitham, S.; Lukoyanov, D. A.; Hoffman, B. M.; Suess, D. L. M., Connecting the Geometric and Electronic Structures of The Nitrogenase Iron–Molybdenum Cofactor through Site-Selective ^{57}Fe Labelling. *Nat. Chem.* **2023**, *15*, 658-665.
- (29) Namkoong, G.; Suess, D. L. M., Cluster-selective ^{57}Fe Labeling of a Twitch-Domain-Containing Radical SAM Enzyme. *Chem. Sci.* **2023**, *14*, 7492-7499.
- (30) Zabret, J.; Bohn, S.; Schuller, S. K.; Arnolds, O.; Möller, M.; Meier-Credo, J.; Liauw, P.; Chan, A.; Tajkhorshid, E.; Langer, J. D.; Stoll, R.; Krieger-Liszkay, A.; Engel, B. D.; Rudack, T.; Schuller, J. M.; Nowaczyk, M. M., Structural Insights into Photosystem II Assembly. *Nat. Plants.* **2021**, *7*, 524-538.
- (31) Sato, A.; Nakano, Y.; Nakamura, S.; Noguchi, T., Rapid-Scan Time-Resolved ATR-FTIR Study on the Photoassembly of the Water-Oxidizing Mn_4CaO_5 Cluster in Photosystem II. *J. Phys. Chem. B* **2021**, *125*, 4031-4045.
- (32) Bao, H.; Burnap, R. L., Photoactivation: The Light-Driven Assembly of the Water Oxidation Complex of Photosystem II. *Front. Plant Sci.* **2016**, *7*, 578.
- (33) Gulam Rabbani, S. M.; Miró, P., Computational Insights into Iron Heterometal Installation in Polyoxovanadate–Alkoxide Clusters. *Inorg. Chem.* **2023**, *62*, 1797-1803.
- (34) Lee, S. C.; Holm, R. H., The Clusters of Nitrogenase: Synthetic Methodology in the Construction of Weak-Field Clusters. *Chem. Rev.* **2004**, *104*, 1135-1158.
- (35) Dobbek, H.; Svetlitchnyi, V.; Gremer, L.; Huber, R.; Meyer, O., Crystal Structure of a Carbon Monoxide Dehydrogenase Reveals a [Ni-4Fe-5S] Cluster. *Science* **2001**, *293*, 1281-1285.
- (36) Suga, M.; Akita, F.; Hirata, K.; Ueno, G.; Murakami, H.; Nakajima, Y.; Shimizu, T.; Yamashita, K.; Yamamoto, M.; Ago, H.; Shen, J.-R., Native Structure of Photosystem II at 1.95 Å Resolution Viewed by Femtosecond X-ray Pulses. *Nature* **2015**, *517*, 99-103.

- (37) Cox, N.; Pantazis, D. A.; Lubitz, W., Current Understanding of the Mechanism of Water Oxidation in Photosystem II and Its Relation to XFEL Data. *Annu. Rev. Biochem* **2020**.
- (38) Suga, M.; Akita, F.; Yamashita, K.; Nakajima, Y.; Ueno, G.; Li, H.; Yamane, T.; Hirata, K.; Umena, Y.; Yonekura, S.; Yu, L.-J.; Murakami, H.; Nomura, T.; Kimura, T.; Kubo, M.; Baba, S.; Kumasaka, T.; Tono, K.; Yabashi, M.; Isobe, H.; Yamaguchi, K.; Yamamoto, M.; Ago, H.; Shen, J.-R., An Oxyl/Oxo Mechanism for Oxygen-Oxygen Coupling in PSII Revealed by an X-ray Free-Electron Laser. *Science* **2019**, *366*, 334.
- (39) Siegbahn, P. E. M., Structures and Energetics for O₂ Formation in Photosystem II. *Acc. Chem. Res.* **2009**, *42*, 1871-1880.
- (40) Ruickoldt, J.; Basak, Y.; Domnik, L.; Jeoung, J.-H.; Dobbek, H., On the Kinetics of CO₂ Reduction by Ni, Fe-CO Dehydrogenases. *ACS Catalysis* **2022**, *12*, 13131-13142.
- (41) Fessler, J.; Jeoung, J.-H.; Dobbek, H., How the [NiFe₄S₄] Cluster of CO Dehydrogenase Activates CO₂ and NCO⁻. *Angew. Chem. Int. Ed.* **2015**, *54*, 8560-8564.
- (42) Bhowmick, A.; Hussein, R.; Bogacz, I.; Simon, P. S.; Ibrahim, M.; Chatterjee, R.; Doyle, M. D.; Cheah, M. H.; Fransson, T.; Chernev, P.; Kim, I.-S.; Makita, H.; Dasgupta, M.; Kaminsky, C. J.; Zhang, M.; Gärtcke, J.; Haupt, S.; Nangca, I. I.; Keable, S. M.; Aydin, A. O.; Tono, K.; Owada, S.; Gee, L. B.; Fuller, F. D.; Batyuk, A.; Alonso-Mori, R.; Holton, J. M.; Paley, D. W.; Moriarty, N. W.; Mamedov, F.; Adams, P. D.; Brewster, A. S.; Dobbek, H.; Sauter, N. K.; Bergmann, U.; Zouni, A.; Messinger, J.; Kern, J.; Yano, J.; Yachandra, V. K., Structural Evidence for Intermediates during O₂ Formation in Photosystem II. *Nature* **2023**, *617*, 629-636.
- (43) Kern, J.; Chatterjee, R.; Young, I. D.; Fuller, F. D.; Lassalle, L.; Ibrahim, M.; Gul, S.; Fransson, T.; Brewster, A. S.; Alonso-Mori, R.; Hussein, R.; Zhang, M.; Douthit, L.; de Lichtenberg, C.; Cheah, M. H.; Shevela, D.; Wersig, J.; Seuffert, I.; Sokaras, D.; Pastor, E.; Weninger, C.; Kroll, T.; Sierra, R. G.; Aller, P.; Butryn, A.; Orville, A. M.; Liang, M.; Batyuk, A.; Koglin, J. E.; Carbajo, S.; Boutet, S.; Moriarty, N. W.; Holton, J. M.; Dobbek, H.; Adams, P. D.; Bergmann, U.; Sauter, N. K.; Zouni, A.; Messinger, J.; Yano, J.; Yachandra, V. K., Structures of the Intermediates of Kok's Photosynthetic Water Oxidation Clock. *Nature* **2018**, *563*, 421-425.
- (44) Nguyen, A. I.; Suess, D. L. M.; Darago, L. E.; Oyala, P. H.; Levine, D. S.; Ziegler, M. S.; Britt, R. D.; Tilley, T. D., Manganese-Cobalt Oxido Cubanes Relevant to Manganese-Doped Water Oxidation Catalysts. *J. Am. Chem. Soc.* **2017**, *139*, 5579-5587.
- (45) Yao, R.; Li, Y.; Chen, Y.; Xu, B.; Chen, C.; Zhang, C., Rare-Earth Elements Can Structurally and Energetically Replace the Calcium in a Synthetic Mn₄CaO₄-Cluster Mimicking the Oxygen-Evolving Center in Photosynthesis. *J. Am. Chem. Soc.* **2021**, *143*, 17360-17365.
- (46) Nguyen, A. I.; Darago, L. E.; Balcells, D.; Tilley, T. D., Influence of a "Dangling" Co(II) Ion Bound to a [MnCo₃O₄] Oxo Cubane. *J. Am. Chem. Soc.* **2018**, *140*, 9030-9033.
- (47) Amtawong, J.; Nguyen, A. I.; Tilley, T. D., Mechanistic Aspects of Cobalt-Oxo Cubane Clusters in Oxidation Chemistry. *J. Am. Chem. Soc.* **2022**.
- (48) Dasgupta, J.; Ananyev, G. M.; Dismukes, G. C., Photoassembly of the Water-Oxidizing Complex in Photosystem II. *Coord. Chem. Rev.* **2008**, *252*, 347-360.
- (49) Vinyard, D. J.; Badshah, S. L.; Riggio, M. R.; Kaur, D.; Fanguy, A. R.; Gunner, M. R., Photosystem II Oxygen-Evolving Complex Photoassembly Displays an Inverse H/D solvent Isotope Effect under Chloride-Limiting Conditions. *Proc. Nat. Acad. Sci. U.S.A.* **2019**, *116*, 18917.
- (50) Xia, X.; Wang, Y.; Ruditskiy, A.; Xia, Y., 25th Anniversary Article: Galvanic Replacement: A Simple and Versatile Route to Hollow Nanostructures with Tunable and Well-Controlled Properties. *Adv. Mater.* **2013**, *25*, 6313-6333.
- (51) Oh, M. H.; Yu, T.; Yu, S.-H.; Lim, B.; Ko, K.-T.; Willinger, M.-G.; Seo, D.-H.; Kim, B. H.; Cho, M. G.; Park, J.-H.; Kang, K.; Sung, Y.-E.; Pinna, N.; Hyeon, T., Galvanic Replacement Reactions in Metal Oxide Nanocrystals. *Science* **2013**, *340*, 964-968.
- (52) Beberwyck, B. J.; Surendranath, Y.; Alivisatos, A. P., Cation Exchange: A Versatile Tool for Nanomaterials Synthesis. *J. Phys. Chem. C* **2013**, *117*, 19759-19770.
- (53) Zhang, D.; Wong, A. B.; Yu, Y.; Brittman, S.; Sun, J.; Fu, A.; Beberwyck, B.; Alivisatos, A. P.; Yang, P., Phase-Selective Cation-Exchange Chemistry in Sulfide Nanowire Systems. *J. Am. Chem. Soc.* **2014**, *136*, 17430-17433.

- (54) Zhang, J.; Wu, Z.; Polo-Garzon, F., Recent Developments in Revealing the Impact of Complex Metal Oxide Reconstruction on Catalysis. *ACS Catalysis* **2023**, 15393-15403.
- (55) Evans, D. F., 400. The Determination of the Paramagnetic Susceptibility of Substances in Solution by Nuclear Magnetic Resonance. *J. Chem. Soc.* **1959**, 2003-2005.
- (56) DeLucia, A. A.; Kelly, K. A.; Herrera, K. A.; Gray, D. L.; Olshansky, L., Intramolecular Hydrogen-Bond Interactions Tune Reactivity in Biomimetic Bis(μ -hydroxo)dicobalt Complexes. *Inorg. Chem.* **2021**, *60*, 15599-15609.
- (57) DeLucia, A. A.; Olshansky, L., Carboxylate Shift Dynamics in Biomimetic $\text{Co}_2(\mu\text{-OH})_2$ Complexes. *Inorg. Chem.* **2024**, *63*, 1109-1118.
- (58) Beattie, J. K.; Hambley, T. W.; Klepetko, J. A.; Masters, A. F.; Turner, P., The Chemistry of Cobalt Acetate—IV. The Isolation and Crystal Structure of the Symmetric Cubane, Tetrakis[(μ -acetato)(μ_3 -oxo) (pyridine)cobalt(III)] · Chloroform Solvate, $[\text{Co}_4(\mu_3\text{-O})_4(\mu\text{-CH}_3\text{CO}_2)_4(\text{C}_5\text{H}_5\text{N})_4] \cdot 5\text{CHCl}$ and of the Dicationic Partial Cubane, Trimeric, [(μ -acetato)(acetato)tris(μ -hydroxy(μ_3 -oxo)hexakispyridinetricobalt(III))hexafluorophosphate · Water Solvate, $[\text{Co}_3(\mu_3\text{-O})(\mu\text{-OH})_3(\mu\text{-CH}_3\text{CO}_2)(\text{CH}_3\text{CO}_2)(\text{C}_5\text{H}_5\text{N})_6][\text{PF}_6]_2 \cdot 2\text{H}_2\text{O}$. *Polyhedron* **1998**, *17*, 1343-1354.
- (59) Beattie, J. K.; Klepetko, J. A.; Masters, A. F.; Turner, P., The Chemistry of Cobalt Acetate. VIII. New Members of the Family of Oxo-Centred Trimers, $[\text{Co}_3(\mu_3\text{-O})(\mu\text{-O}_2\text{CCH}_3)_{5-p}(\mu\text{-OR})_p\text{L}_5]^{2+}$ (R=H, alkyl, L=ligand, p=0–4). The Preparation and Characterisation of the Trimeric tetrakis(μ -acetato)-(μ -hydroxo)- μ_3 -oxo-pentakis(pyridine)-tri-cobalt(III) hexafluorophosphate, $[\text{Co}_3(\mu_3\text{-O})(\mu\text{-O}_2\text{CCH}_3)_4(\mu\text{-OH})(\text{C}_5\text{H}_5\text{N})_5][\text{PF}_6]_2$, and the Preparation and Crystal Structure of the Trimeric tris(μ -acetato)-(μ -hydroxo)-(μ -methoxo)- μ_3 -oxo-pentakis(pyridine)-tri-cobalt(III) Hexafluorophosphate·Methanol·Water Solvate $[\text{Co}_3(\mu_3\text{-O})(\mu\text{-O}_2\text{CCH}_3)_3(\mu\text{-OH})(\mu\text{-OCH}_3)(\text{C}_5\text{H}_5\text{N})_5][\text{PF}_6]_2 \cdot \text{CH}_3\text{OH} \cdot 0.25\text{H}_2\text{O}$. *Polyhedron* **2003**, *22*, 947-965.
- (60) Snider, B. B.; Patricia, J. J.; Kates, S. A., Mechanism of Manganese(III)-Based Oxidation of β -Keto Esters. *The Journal of Organic Chemistry* **1988**, *53*, 2137-2143.
- (61) Tategami, S.-i.; Yamada, T.; Nishino, H.; Korp, J. D.; Kurosawa, K., Formation of 1,2-Dioxacyclohexanes by the Reaction of Alkenes with Tris(2,4-pentanedionato)manganese(III) or with β -Ketocarbonyl Compounds in the Presence of Manganese(III) Acetate. *Tetrahedron Lett.* **1990**, *31*, 6371-6374.
- (62) Melikyan, G. G., Carbon–Carbon Bond-Forming Reactions Promoted by Trivalent Manganese. In *Organic Reactions*, 2004; pp 427-675.
- (63) Nishino, H., Direct Diacetylmethylation of Aromatic Compounds with Tris(2,4-pentanedionato)manganese(III). *Bull. Chem. Soc. Jpn.* **1986**, *59*, 1733-1739.
- (64) Goff, H. M.; Hines, J.; Griesel, J.; Mossman, C., Synthesis, Characterization, and use of a Cobalt(II) Complex as an NMR shift Reagent: An Integrated Laboratory Experiment. *J. Chem. Educ.* **1982**, *59*, 422.
- (65) Chakrabarty, R.; Bora, S. J.; Das, B. K., Synthesis, Structure, Spectral and Electrochemical Properties, and Catalytic Use of Cobalt(III)–Oxo Cubane Clusters. *Inorg. Chem.* **2007**, *46*, 9450-9462.
- (66) Nguyen, A. I.; Wang, J.; Levine, D. S.; Ziegler, M. S.; Tilley, T. D., Synthetic Control and Empirical Prediction of Redox Potentials for Co_4O_4 Cubanes over a 1.4 V Range: Implications for Catalyst Design and Evaluation of High-valent Intermediates in Water Oxidation. *Chem. Sci.* **2017**, *8*, 4274-4284.
- (67) Amtawong, J.; Skjelstad, B. B.; Balcells, D.; Tilley, T. D., Concerted Proton–Electron Transfer Reactivity at a Multimetallic Co_4O_4 Cubane Cluster. *Inorg. Chem.* **2020**, *59*, 15553-15560.
- (68) Gritzner, G.; Murauer, H.; Gutmann, V., The Polarographic and Voltammetric Behaviour of Acetylacetonato and Hexafluoroacetylacetonato Complexes in Acetonitrile. *Journal of Electroanalytical Chemistry and Interfacial Electrochemistry* **1979**, *101*, 177-183.
- (69) Gritzner, G.; Murauer, H.; Gutmann, V., Solvent and Salt Effects on the Redox Behaviour of Trisacetylacetonato manganese(III). *Journal of Electroanalytical Chemistry and Interfacial Electrochemistry* **1979**, *101*, 185-200.
- (70) Carli, S.; Benazzi, E.; Casarin, L.; Bernardi, T.; Bertolasi, V.; Argazzi, R.; Caramori, S.; Bignozzi, C. A., On the Stability of Manganese Tris(β -diketonate) Complexes as Redox Mediators in DSSCs. *PCCP* **2016**, *18*, 5949-5956.
- (71) Taube, H.; Myers, H.; Rich, R. L., Observations on the Mechanism of Electron Transfer in Solution. *J. Am. Chem. Soc.* **1953**, *75*, 4118-4119.

(72) Taube, H., Electron Transfer Between Metal Complexes: Retrospective. *Science* **1984**, 226, 1028-1036.

(73) Burdett, J. K., A Molecular Orbital Approach to Electron-Transfer Reactions between Transition-Metal Ions in Solution. *Inorg. Chem.* **1978**, 17, 2537-2552.

(74) Haim, A., Role of the Bridging Ligand in Inner-Sphere Electron-Transfer Reactions. *Acc. Chem. Res.* **1975**, 8, 264-272.

(75) Thompson, G. A. K.; Sykes, A. G., Assignment of Mechanism to Titanium(III) Reductions of Cobalt(III) complexes. Hard and Soft Theory as a Means of Assessing Bridging Ligands for Inner-Sphere Electron Transfer. *Inorg. Chem.* **1976**, 15, 638-642.

(76) Taube, H.; Gould, E. S., Organic Molecules as Bridging Groups in Electron-Transfer Reactions. *Acc. Chem. Res.* **1969**, 2, 321-329.

(77) Zhang, D.; Yang, Y.; Bekenstein, Y.; Yu, Y.; Gibson, N. A.; Wong, A. B.; Eaton, S. W.; Kornienko, N.; Kong, Q.; Lai, M.; Alivisatos, A. P.; Leone, S. R.; Yang, P., Synthesis of Composition Tunable and Highly Luminescent Cesium Lead Halide Nanowires through Anion-Exchange Reactions. *J. Am. Chem. Soc.* **2016**, 138, 7236-7239.

(78) Murray, J. W.; Rutherford, A. W.; Nixon, P. J., Photosystem II in a State of Disassembly. *Joule* **2020**, 4, 2082-2084.

(79) da Silva, A. G. M.; Rodrigues, T. S.; Haigh, S. J.; Camargo, P. H. C., Galvanic Replacement Reaction: Recent Developments for Engineering Metal Nanostructures Towards Catalytic Applications. *Chem. Commun.* **2017**, 53, 7135-7148.

Graphical Abstract

